Biosensors

Deutsche Ausgabe: DOI: 10.1002/ange.201800485
Internationale Ausgabe: DOI: 10.1002/anie.201800485

A Multi-signal Fluorescent Probe with Multiple Binding Sites for Simultaneous Sensing of Cysteine, Homocysteine, and Glutathione

Guo-xing Yin, Ting-ting Niu, Ya-bing Gan, Ting Yu, Peng Yin, Hai-min Chen,* You-yu Zhang, Hai-tao Li,* and Shou-zhuo Yao*

Abstract: *A novel fluorescent probe was developed by integrating chlorinated coumarin and benzothiazolylacetonitrile and exploited for simultaneous detection of cysteine (Cys), homocysteine (Hcy), and glutathione (GSH). Featuring four binding sites and different reaction mechanisms for different biothiols, this probe exhibited rapid fluorescence turn-on for distinguishing Cys, Hcy, and GSH with 108-, 128-, 30-fold fluorescence increases at 457, 559, 529 nm, respectively, across different excitation wavelengths. Furthermore, the probe was successfully applied to the fluorescence imaging of endogenous Cys and GSH and exogenous Cys, Hcy, and GSH in living cells.*

Small-molecule thiols play vital roles in many physiological processes and are closely related to a lot of diseases.[1] Cysteine (Cys), homocysteine (Hcy), and glutathione (GSH) are amongst the most abundant and important biological thiols. Though they have the similar structures and reactivity, the roles played by Cys, Hcy, and GSH are totally different. Cys is an essential amino acid for the synthesis of proteins, and abnormal levels of Cys are related to such conditions as edema, slowed growth in children, lethargy, cardiovascular diseases, liver damage.[2] The role of Hcy in diseases remains a highly contentious topic.[3] Its normal concentration in serum is approximately 5–15 μM and abnormal total homocysteine might cause cognitive impairment in the elderly.[4] GSH is well-known to be associated with a series of disorders including cancer and Alzheimer's disease.[5] Considering the important biological roles of biothiols and the relationship of many diseases with changes in their concentrations (intracellular concentration for Cys: 30–200 μM;[6] for GSH: 1–10 mM[5]), it is of great value to develop effective methods for real-time simultaneous monitoring of intracellular Cys, Hcy, and GSH, respectively, in biological systems.

[*] G. Yin, Y. Gan, T. Yu, Dr. P. Yin, Prof. Y. Zhang, Prof. T. Li, Prof. S. Yao
Key Laboratory of Chemical Biology and Traditional Chinese Medicine Research (Ministry of Education), College of Chemistry and Chemical Engineering, Hunan Normal University
Changsha 410081 (China)
E-mail: yinpeng@hunnu.edu.cn
haitao-li@hunnu.edu.cn
T. Niu, Prof. H. Chen
Key Laboratory of Marine Biotechnology of Zhejiang Province
Ningbo University, Ningbo, Zhejiang 315211 (P. R. China)
E-mail: chenhaimin@nbu.edu.cn
Supporting information and the ORCID identification number(s) for the author(s) of this article can be found under: https://doi.org/10.1002/anie.201800485.

High-performance liquid chromatography (HPLC), mass spectrometry (MS), capillary electrophoresis, and HPLC-MS/MS have been applied to the detection and determination of specific biothiols.[7] Recently, owing to their non-invasiveness, high selectivity, high sensitivity, relative low cost and operational simplicity, a large number of fluorescent probes have been developed to detect and sense biothiols.[8] Despite similarity among the structures and properties of Cys, Hcy and GSH, several fluorescent probes that allow selective detection of two species at one time have been reported.[9] However, it is more challenging to discriminate the three thiols from each other simultaneously. Guo and co-workers have developed a chlorinated coumarin–hemicyanine probe with three potential reaction sites for simultaneous detection of Cys and GSH from different emission channels.[10] Although the signaling promoted by Hcy was poor and 60 min was needed for the sensing, their work exhibits an excellent perspective for simultaneous Cys/Hcy/GSH detection. Liang and co-workers have also reported a sulfonamide-based self-quenched fluorescent probe for simultaneous detection of biothiols.[11] Each product for the probe with Cys/Hcy/GSH exhibited different emission maxima, but the difference between the emissions with Cys and Hcy was very small (5 nm) and the probe required 2 h at 37 °C for the detection. In 2016, Sun and co-workers developed a commercial fluorescent probe (2,3,5,6-tetrafluoro-terephthalonitrile) for differentiating Cys, Hcy, and GSH in living cells.[12] Although the probe has four potential reaction sites for detecting biological thiols, long sensing time (up to 2 h) was needed to reach an optimal signal and the addition of CTAB (cetyl trimethylammonium bromide) was required to discriminate Hcy from GSH, which are significant barriers to the simultaneous monitoring of Cys, Hcy and GSH in living cells. Simultaneous analysis of biothiols (Cys/Hcy/GSH) in vivo/vitro from different emission channels with a single-molecule fluorescent probe, which is still quite rare, would be highly valuable but even more challenging. Herein, we presented a novel fluorescent probe with four potential reaction sites for simultaneous and rapid sensing of Cys, Hcy, and GSH from three emission channels based on different reaction mechanisms between probe and biothiols (Scheme 1). This probe was capable of not only fluorescence imaging of exogenous Cys, Hcy, and GSH but also simultaneous detection of endogenous Cys and GSH from different emission channels in living cells. Furthermore, it has great potential for real-time simultaneous and quantitative monitoring of cellular Cys, Hcy, and GSH, which will greatly promote the clarification of their complicated relationship and functions in various physiological processes.

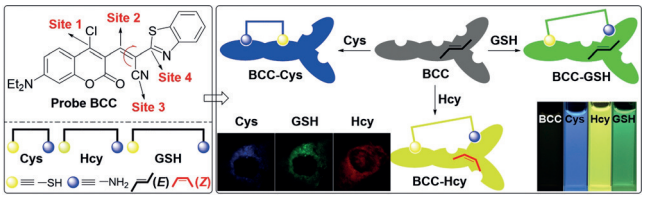

Scheme 1. Simultaneous sensing of Cys, Hcy, and GSH based on the four binding sites of probe BCC.

Probe BCC was rationally designed with four potential reaction sites, using coumarin as a fluorophore (Scheme 1). A number of structural features contribute to the activity of the probe. The chlorine atom in the 4-position of the coumarin moiety (site 1) is reactive and facilitates the thiol–halogen S_NAr nucleophilic aromatic substitution between probe BCC and thiols. The α,β-unsaturated bond (site 2) is a well-known Michael acceptor. The cyano group could be utilized as an electrophile (site 3), and under the effect of the cyano group, the unsaturated bond in the benzothiazolium moiety could be used to another reaction site (site 4) for discriminating biothiols. The steric distance between thiol group and amino group in biothiols should be: Cys < Hcy < GSH (Scheme S1 in the Supporting Information). A probe with four potential reaction sites at different steric distances should enable discrimination of similar biothiols.

Initially, we synthesized probe BCC (see the Supporting Information) and examined its sensing behavior towards Cys/Hcy/GSH by using time-dependent UV/Vis and fluorescence spectroscopy in DMSO/PBS (pH 7.4, 10 mM, v/v, 6/4) at room temperature. As shown in Figure 1, the UV/Vis spectra of free BCC show a main absorption at 500 nm ($\varepsilon = 3.86 \times 10^4\ L\,mol^{-1}\,cm^{-1}$, quantum yield (QY) = 0.003, with Rhodamine B as reference). Upon addition of Cys, the initial absorption peak at 500 nm decreased dramatically while a new peak at 374 nm appeared with a 126 nm blue shift (Figure 1a and Figure S1 in the Supporting Information), which indicated that the conjugation between the coumarin and benzothiazolylacetonitrile is broken due to the Michael addition of Cys to site 2 in the probe. This likely corresponds to the formation of product BCC–Cys, which has a seven-membered ring (QY = 0.313, with quinine sulfate as reference; Scheme S3a). Correspondingly, a significant fluorescence turn-on with 108-fold enhancement at 457 nm was observed in time-dependent fluorescence spectra at 360 nm excitation within 15 min, but there was only a slight fluorescence enhancement for Hcy (3.5-fold), GSH (11-fold), and NAC (N-Acetylcysteine) (1.2-fold) under the same condition (Figure 2a,b and Figures S5, S6).

For Hcy, the time-dependent UV/Vis spectrum is similar to Cys in the first 2 min, with a decrease of the initial absorption peak at 500 nm and a simultaneous increase of

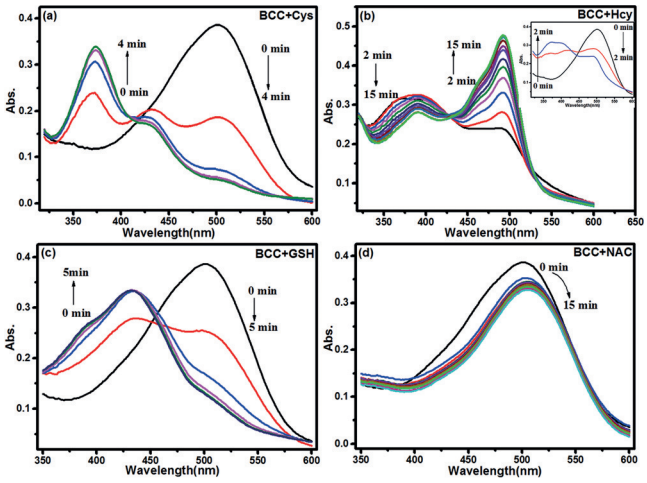

Figure 1. a–d) Time-dependent absorption spectra of BCC (10 μM) in the presence of 10 equiv of Cys (a), Hcys (b), GSHs (c), and NACs (d) in DMSO/PBS (pH 7.4, 10 mM, v/v, 6/4) at RT. DMSO = dimethyl sulfoxide, PBS = phosphate-buffered saline.

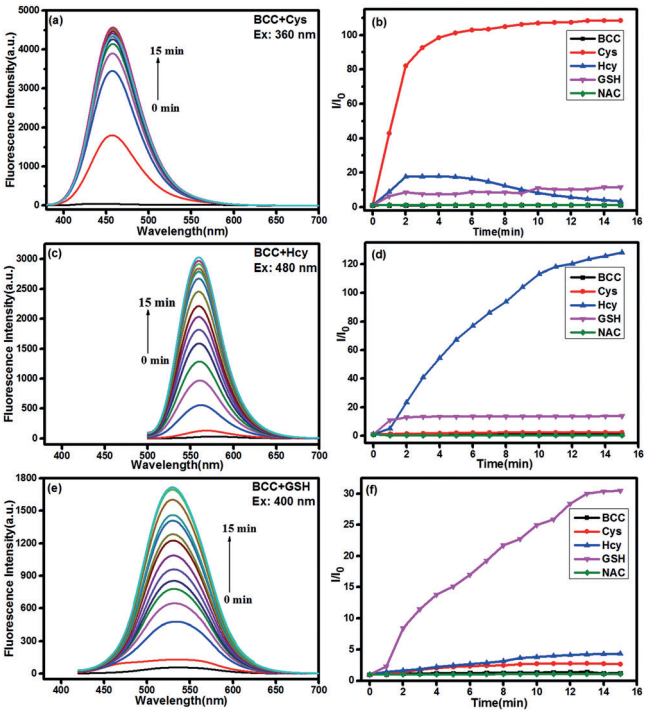

Figure 2. a, c, e) Time-dependent fluorescence spectra of BCC (10 μM) in the presence of 10 equiv of Cys excited at 360 nm (a), 10 equiv of Hcy excited at 480 nm (c), 10 equiv of GSH excited at 400 nm (e). b, d, f) Time-dependent fluorescence intensity changes toward 10 equiv of biothiols excited at 360 nm (b), 480 nm (d), and 400 nm (f). Condition: DMSO/PBS (pH 7.4, 10 mM, v/v, 6/4) at room temperature. Slit (nm): 2.5/2.5.

a new broad absorption peak at 391 nm (insert, Figure 1b). After that, the absorption at 391 nm showed a slight decrease and a new peak at 492 nm increased slowly and reached a plateau after 15 min (Figure S2). The absorption at 391 nm is assigned to an intermediate, which was further transferred to the final product BCC–Hcy (QY = 0.474, with Rhodamine B as reference). Configuration changes (from *E* to *Z*) of the intermediate might take place, which would be favorable for the addition of a free amine group to the cyano group (Scheme S3b). Supported by the fluorescence color changes and the time-dependent fluorescence spectra at 360 nm excitation, the slight emission at 444 nm decreased slowly

after 2 min and emission at 559 nm was enhanced (Figure S6). More importantly, a large fluorescence turn-on at 559 nm with 128-fold enhancement was observed ($\lambda_{ex} = 480$ nm; Figure 2c,d), and the fluorescence enhancement at 559 nm ($\lambda_{ex} = 480$ nm) for Cys (2.4-fold), GSH (13.7-fold), and NAC (0.2-fold) could be neglected (Figure S7).

We continued to investigate the performance of the probe with GSH. As shown in Figure 1c (details in Figure S3), the initial absorption peak at 500 nm decreased dramatically after the addition of GSH, and a new absorption peak was found at 432 nm with a 68 nm blue shift, which indicated nucleophilic addition of the amine group in GSH to site 4 in probe BCC (Scheme S3c). As a model compound of amino-free thiols, NAC was also tested and the initial absorption decreased slightly probably due to a thioether substitution (Figure 1d, Scheme S3d, and Figure S4). The time-dependent fluorescence spectra for the probe with GSH ($\lambda_{ex} = 360$ and 480 nm) exhibited weak fluorescence (Figures S5 and S7), but a 30-fold fluorescence enhancement at 529 nm was achieved ($\lambda_{ex} =$ 400 nm; QY = 0.097, with quinine sulfate as reference), while, Cys, Hcy, and NAC displayed less than 5-fold fluorescence enhancement at 529 nm (Figure 2e,f and Figure S8). Furthermore, probe BCC exhibited little fluorescence ($\lambda_{ex} =$ 360, 400 and 480 nm, respectively) and was stable for a long time (Figure S9).

Taken together, the results from spectral studies demonstrate that probe BCC can distinguish between Cys, Hcy, and GSH through different fluorescence signals, and shows excellent performances for sensing biothiols (Table S1). Encouraging by these results, we further evaluated the selectivity of probe BCC over other biological species, including various amino acids and representative anions (Figures S10–S12). Only Cys, Hcy, and GSH promoted obvious fluorescence intensity enhancement at 457, 559, and 529 nm ($\lambda_{ex} = 360$, 480, and 400 nm, respectively) within a short time (15 min), thus confirming the excellent selectivity of probe BCC for Cys, Hcy, and GSH. Furthermore, results from the detection of Cys, Hcy, and GSH in a mixture of the three biothiols demonstrated that probe BCC can be applied to simultaneously sensing of Cys, Hcy, and GSH in complex biological environments (Figures S16–S23).

In addition, fluorescence titration experiments under the same conditions were conducted. As shown in Figures S13–S15, an excellent linear relationship from 0–3 equiv of Cys was obtained and the detection limit was calculated to be as low as 0.5 nM based on S/N = 3. The fluorescence intensities were linearly proportional to the amount of Hcy and GSH from 0 to 2 equiv, and the detection limits were calculated as 3.6 nM and 6.9 nM, respectively. In view of these results, probe BCC could be applied to sense intracellular biothiols.

Next, to investigate the reaction mechanism between probe BCC and Cys/Hcy/GSH, products of BCC–Cys, BCC–Hcy, and BCC–GSH were observed in HRMS titration experiments (Figures S38–S40). Although the isolation of products BCC–Cys and BCC–GSH failed, the product BCC–Hcy was successfully obtained and characterized. We can thus propose a reaction mechanism for probe BCC with biothiols (Scheme 2 and Scheme S3), which was based on spectral studies and NMR analyses (Figures S24, S25, S36–S47). Based on the four binding sites in the probe and the differences in the structures of Cys, Hcy, and GSH, compounds with different photophysical properties would be expected to be formed after reactions between probe BCC and Cys, Hcy, and GSH respectively. Further mechanistic studies are still in progress in our laboratory.

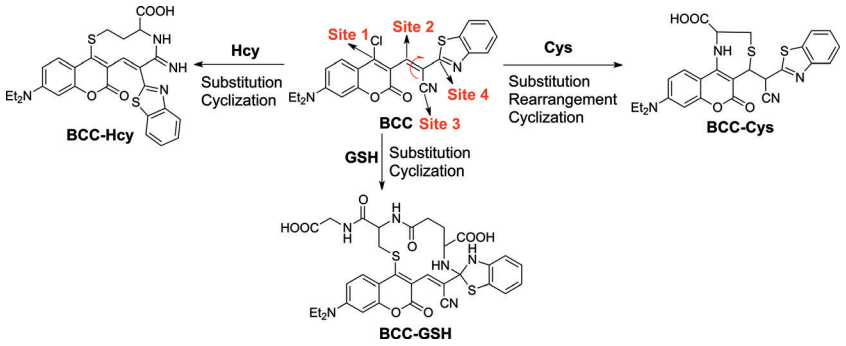

Scheme 2. Proposed reaction mechanisms of probe BCC with Cys, Hcy, and GSH.

Subsequently, the ability of probe BCC to selectively sense exogenous and intercellular Cys, Hcy, and GSH was evaluated. Firstly, the results from MTT assays showed that probe BCC has good cell permeability and low cytotoxicity to living cells over a short period of time (Figure S26). For exogenous biothiols, the cells were firstly pretreated with NEM, and cellular biothiols and SH-containing proteins were deactivated. After incubation with probe BCC, almost no fluorescence could be observed (Figure S27, A1–A3). In contrast, following treatment with Cys, Hcy, and GSH, we observed blue, red, and green fluorescence, respectively, from three different emission channels in living cells with high selectivity (Figure 3, C1–C3 and Figure S27). Fluorescence images for BEL-7402 cells with different concentrations of exogenous Cys (or GSH) were also conducted, and the differences in fluorescence intensities indicate the different concentrations of Cys/GSH in living cells (Figure S28).

For imaging of cellular biothiols, cells incubated without probe BCC exhibited almost no fluorescence (Figure 3, A1–A3). After incubation with probe BCC for 30 min, BEL-7402 cells exhibited different blue fluorescence for Cys detection and green fluorescence for GSH detection. Almost no red fluorescence for Hcy was observed, which may be due to the low concentration of Hcy in living cells (Figure 3, B1–B3). Fluorescence images for cellular Cys and GSH in different kinds of cells were further performed (Figure S29). Thus, this probe could be further applied to the real-time quantitative monitoring of cellular Cys and GSH.

In summary, we have designed and synthesized a novel chlorinated coumarin–benzothiazolium fluorescent probe (BCC) with four binding sites, which can simultaneously and selectively detect Cys, Hcy, and GSH in three different emission channels. The fluorescence increments of probe BCC for Cys, Hcy, and GSH at 457, 559, and 529 nm are 108-,

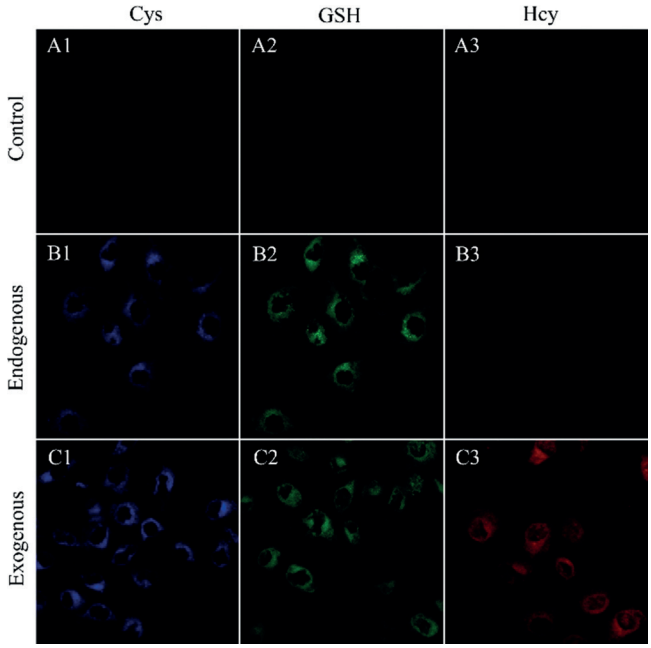

Figure 3. Confocal fluorescence images of Cys, GSH, and Hcy in BEL-7402 cells. A1–A3) Cells were incubated for 30 min, then imaged. B1–B3) Cells were incubated with probe BCC (2.5 μM) for 30 min, then imaged. C1–C3) Cells were pretreated with NEM (0.5 mM, 30 min), subsequently incubated with Cys/GSH/Hcy (500 μM, 30 min) and probe BCC (2.5 μM, 30 min), then imaged (λ_{ex} = 405 nm, λ_{em} = 421–475 nm for the blue channel; λ_{ex} = 458 nm, λ_{em} = 500–550 nm for the green channel; and λ_{ex} = 543 nm, λ_{em} = 552–617 nm for the red channel). Scale bar: 20 μm.

128-, and 30-fold increases (λ_{ex} = 360, 480, and 400 nm), respectively, based on different reaction mechanisms, with high selectivity and high sensitivity. Furthermore, fluorescence imaging studies in different living cells demonstrated that probe BCC can be used to simultaneously monitor endogenous Cys and GSH and exogeneous Cys, Hcy, and GSH through multicolor imaging. This study could pave the way for further exploration of the cellular dynamics of biothiols and their function in biological systems, thereby promoting the investigation of biothiols in biomedicine and diagnostics.

Acknowledgements

This work was supported by the funding from the National Natural Science Foundation of China (Grant No. 21405043, 21675051 and 81370532), K.C. Wong Magna Fund in Ningbo University, LiDakSum Marine Biopharmaceutical Development Fund and Opening Fund of Key Laboratory of Chemical Biology and Traditional Chinese Medicine Research (Ministry of Education of China), Hunan Normal University.

Conflict of interest

The authors declare no conflict of interest.

Keywords: biosensors · cysteine · fluorescent probes · glutathione · thiols

How to cite: *Angew. Chem. Int. Ed.* **2018**, *57*, 4991–4994
Angew. Chem. **2018**, *130*, 5085–5088

[1] a) Z. A. Wood, E. Schroder, J. Robin Harris, L. B. Poole, *Trends Biochem. Sci.* **2003**, *28*, 32–40; b) T. V. Mishanina, M. Libiad, R. Banerjee, *Nat. Chem. Biol.* **2015**, *11*, 457–464; c) S. Zhang, C.-N. Ong, H.-M. Shen, *Cancer Lett.* **2004**, *208*, 143–153.
[2] a) Y. Zhang, X. Shao, Y. Wang, F. Pan, R. Kang, F. Peng, Z. Huang, W. Zhang, W. Zhao, *Chem. Commun.* **2015**, *51*, 4245–4248; b) S. Shahrokhian, *Anal. Chem.* **2001**, *73*, 5972–5978.
[3] B. Debreceni, L. Debreceni, *Cardiovasc. Ther.* **2014**, *32*, 130–138.
[4] H. Y. Lee, Y. P. Choi, S. Kim, T. Yoon, Z. Guo, S. Lee, K. M. K. Swamy, G. Kim, J. Y. Lee, I. Shin, J. Yoon, *Chem. Commun.* **2014**, *50*, 6967–6969.
[5] C. Hwang, A. Sinskey, H. Lodish, *Science* **1992**, *257*, 1496–1502.
[6] Y. Yue, F. Huo, P. Ning, Y. Zhang, J. Chao, X. Meng, C. Yin, *J. Am. Chem. Soc.* **2017**, *139*, 3181–3185.
[7] a) J. Vacek, B. Klejdus, J. Petrlova, L. Lojkova, V. Kuban, *Analyst* **2006**, *131*, 1167–1174; b) T. Inoue, J. R. Kirchhoff, *Anal. Chem.* **2002**, *74*, 1349–1354; c) M. J. MacCoss, N. K. Fukagawa, D. E. Matthews, *Anal. Chem.* **1999**, *71*, 4527–4533; d) B. Seiwert, U. Karst, *Anal. Chem.* **2007**, *79*, 7131–7138.
[8] a) X. Chen, Y. Zhou, X. Peng, J. Yoon, *Chem. Soc. Rev.* **2010**, *39*, 2120–2135; b) J. Chan, S. C. Dodani, C. J. Chang, *Nat. Chem.* **2012**, *4*, 973–984; c) H. S. Jung, X. Chen, J. S. Kim, J. Yoon, *Chem. Soc. Rev.* **2013**, *42*, 6019–6031; d) L.-Y. Niu, Y.-Z. Chen, H.-R. Zheng, L.-Z. Wu, C.-H. Tung, Q.-Z. Yang, *Chem. Soc. Rev.* **2015**, *44*, 6143–6160; e) C.-X. Yin, K.-M. Xiong, F.-J. Huo, J. C. Salamanca, R. M. Strongin, *Angew. Chem. Int. Ed.* **2017**, *56*, 13188–13198; *Angew. Chem.* **2017**, *129*, 13368–13379.
[9] a) O. Rusin, N. N. St. Luce, R. A. Agbaria, J. O. Escobedo, S. Jiang, I. M. Warner, F. B. Dawan, K. Lian, R. M. Strongin, *J. Am. Chem. Soc.* **2004**, *126*, 438–439; b) X. Yang, Y. Guo, R. M. Strongin, *Angew. Chem. Int. Ed.* **2011**, *50*, 10690–10693; *Angew. Chem.* **2011**, *123*, 10878–10881; c) Y. Yue, F. Huo, X. Li, Y. Wen, T. Yi, J. Salamanca, J. O. Escobedo, R. M. Strongin, C. Yin, *Org. Lett.* **2017**, *19*, 82–85; d) L.-Y. Niu, Y.-S. Guan, Y.-Z. Chen, L.-Z. Wu, C.-H. Tung, Q.-Z. Yang, *J. Am. Chem. Soc.* **2012**, *134*, 18928–18931; e) S.-Y. Lim, K.-H. Hong, D. I. Kim, H. Kwon, H.-J. Kim, *J. Am. Chem. Soc.* **2014**, *136*, 7018–7025; f) W. Chen, H. Luo, X. Liu, J. W. Foley, X. Song, *Anal. Chem.* **2016**, *88*, 3638–3646; g) Q. Hu, C. Yu, X. Xia, F. Zeng, S. Wu, *Biosens. Bioelectron.* **2016**, *81*, 341–348; h) L. He, X. Yang, K. Xu, X. Kong, W. Lin, *Chem. Sci.* **2017**, *8*, 6257–6265.
[10] J. Liu, Y.-Q. Sun, Y. Huo, H. Zhang, L. Wang, P. Zhang, D. Song, Y. Shi, W. Guo, *J. Am. Chem. Soc.* **2014**, *136*, 574–577.
[11] Q. Miao, Q. Li, Q. Yuan, L. Li, Z. Hai, S. Liu, G. Liang, *Anal. Chem.* **2015**, *87*, 3460–3466.
[12] H. Zhang, R. Liu, J. Liu, L. Li, P. Wang, S. Q. Yao, Z. Xu, H. Sun, *Chem. Sci.* **2016**, *7*, 256–260.

Manuscript received: January 12, 2018
Revised manuscript received: February 20, 2018
Accepted manuscript online: March 7, 2018
Version of record online: March 22, 2018

